

Optimization of Heat Transfer Rate of Thermal Chimney by Variation in Geometry

Kuldeep Dehariya

M.Tech Scholar

Department of Mechanical Engineering

NRI Institute of Research & Technology

Bhopal (M.P.), India

dehariya.karan73@gmail.com

Prof. Sunil Kumar Chatruvedi

Assistant Professor

Department of Mechanical Engineering

NRI Institute of Research & Technology

Bhopal (M.P.), India

Abstract: A solar chimney is a type of thermal ventilation system that is powered by the sun. It is a strategy for enhancing natural ventilation and also supplying heating and cooling inside a constructing by leveraging energy from the sun to enhance natural stack effect ventilation throughout a building. It can also be used to generate renewable energy. This paper describes the designing of thermal chimney and effect of temperature, velocity and pressure in the three different scenarios

Keywords: Thermal Chimney, CFD, Condenser, Thermal heat.

I. INTRODUCTION

Solar chimneys are a simple and cost-effective way to warm and evacuate a structure. To begin, a chimney must be constructed and encapsulated in a dark or black substance. It's black since it limits the burden of sunlight throwback off the chimney, allowing it to suck more heat and handover it to the air within the tower. In addition, if the residence is in the Northern Hemisphere, such chimneys are normally installed on a south-facing surface.

The procedure of employing a solar chimney to thermal a space is relatively simple. The section of air within the chimney is warmed up even before radiation from the sun strikes the aspect of the chimney. The warmed air is throwback into the living areas if the upper outer ventilation systems of the chimney are shutdown. This creates a convection atmosphere heating effect. As the atmosphere in the room starts to cool, it is dragged back into the solar chimney, where it is heated once more. Solar chimneys work in a similar way to Trombe walls if used for warming.

The cooling of a space with a solar chimney differs slightly from the cooling of a space with a Trombe wall. Two vents are available because a roof overhang could be implemented in addition to a thermal chimney. The upper section of the chimney's initial vent has already been noted. The second is on the reverse side of the structure, supplying an air circulation entering among the tower and the exterior air. The column of air within the chimney is warmed as well when solar radiation starts hitting the aspect of the chimney. The upper section of the chimney's vent is maintained to prevent this warm air from becoming entangled.

To start creating favourable environment from within building structures, passive design helps to maximize the usage of 'natural' source materials of heaters, refrigeration, and air conditioning. The internal factors is controlled by ecologic factors included as solar irradiance, cool evening air, and pressurisation discrepancies. Electromechanical systems are not used in passive strategies.

II. LITERATURE REVIEW

(2020, W. Li et al.) [1] Under 22.5 air temperatures, the coupled temperature distribution in a specially built thermal flue with eleven electronic heating systems was probed utilising CFD code-ANSYS 2019R CFX at varied heater negligible temps based on steady 3D Analytical solution and k multiple velocity components as well as Nonlinear floatation presumption. The chimney's overarching heat transfer, heat transfer rate, temp, and stream pastures were all thoroughly investigated. The effect of the heaters' radioactivity on the air in the chimney was considered. The axial ambient temperature of the varying temperature characteristics on the heated wall was plotted, CEL was used to design and enforce thermal continuity equation in CFX-Pre. Our PIV metrics in the semi aircraft cross the heating systems at three heating element nominal temps were used to verify the fluid flows in the chimney. The predicted Nusselt number was compared with existing comparisons in the literary works.

(Dhahri and colleagues, 2021) [2] In this study, four different setups of an altered wall absorbing material with a photovoltaic panel are tested. Cfd model is used to solve the model, which include the consistency, dynamism, and energy equations. The factors of liquid flow and temperature character traits within the solar chimney were subjected to identification and quantification. The impacts of the multiple altered wall absorbers, as well as the severity of solar irradiance, on exergy analysis effectiveness, were investigated. The assessments used in this study enabled the best absorption wall setup to be discovered.

(Wang & Lei, 2020) (Wang & Lei, 2020) (Wang & Lei, 2020) (Wang The effectiveness of a solar pv flue and liquid line systems in the context of airflow, equaled temp, and hot water is investigated in this study through a sequence of experiments conducted. The impact of significant design parameters such as air separation distance, water depth depth, and glass

window depth on the combined system's performance is investigated. Ground tinting's impacts at various locations are also investigated. The data found from Computational fluid dynamics are compared from the ridiculously simplistic THBM established.

2020 (Khidhir & Atrooshi) [4] The impact of concentrated solar density was applied to an altered solar air heater layout in this study. The exploratory rig's rather unusual configuration was designed to test a number of factors, which include design features, reduced size, and implementation in areas with limited natural land inclination. The enquiry also included experimental and analytical work designed to improve the system's growth by enhancing solar density using a traceability diffuser and a transceiver plate. The optimum heat transfer without the impact of density at the foundation of the flue for a chosen day in January was 10.85 °C, acquired at 14:00 hrs. . With simulink assessment in Matlab, the capacity to replicate the experimentally obtained outcomes was tested for chosen months to January, February, and April of 2018. With a mean difference of 7.0 percent, the best designed to match was discovered for the time period 9 to 14 hours.

(Mehdipour and colleagues, 2020) [5] A new indoor testing procedure is used to investigate the solar air heater collector's stable thermal efficiency while minimising the influence of natural adjustments on the exams. The findings will aid in the development of future of solar chimneys, which will have improved geometrical and heating value. Large heat and coefficient of friction losses caused by eddy currents cause less than 9% of the electricity to enter the flue and make electricity, according to the findings. The hoarder angle is known to be the most essential property in attempting to control two - phase flow creation. Enhancing the hoarder angle from 0 to 14 reduces heat resistance by 1.72 percent and improves the rate of heat transfer by 41.6 percent for the differing hoarder.

III. METHODOLOGY

The principal measurements of a thermoelectric fireplace with a hexagonal pass of around the were designed and constructed, as seen in Fig. 1. The flue is mainly composed of four 5 mm in thickness perspex layers held together by two aluminium. One row of gaps in a couple of sheets allows for the installation of 12 conical electronic heating systems with a diameter of 16 mm(d) and a length of 200 mm. These heating systems serve as a primary heat transfer fluid heater and are controlled by an OMEGATM PID (proportional integral derivative) gamepad to maintain a consistent reheat temperature increase. The second heat exchanger's underside row of gaps is overlooked and not designed to simulate. The lateral bullet heating systems are spread fairly, with an optimum solution centre-to-centre range of 1.75d, which was ascertained using 2D CFD heat exchange simulation models in (Ma et al., 2019).

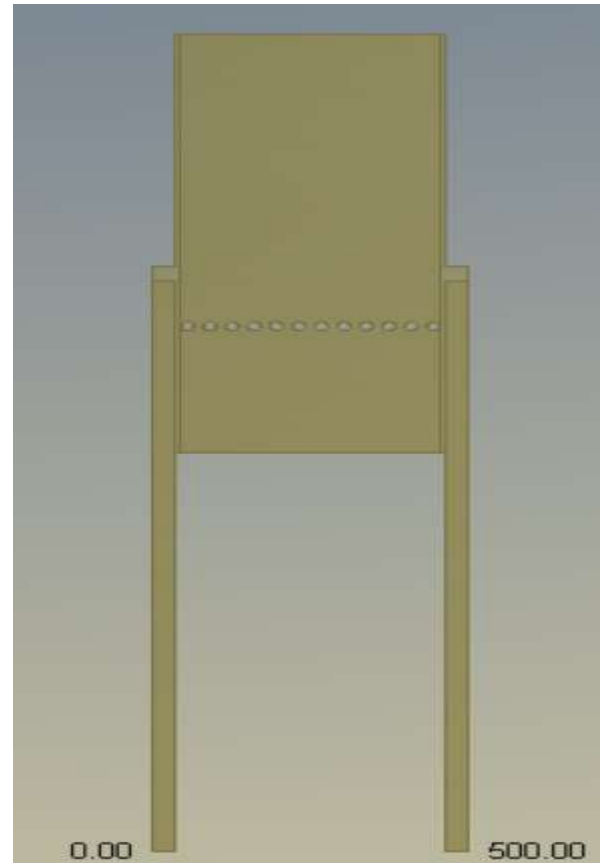


Figure 1 CAD Model of Chimney

The chimney distances along each heaters, including both, are 32.5d and 12.5d. Table 1 lists the tangible asset constant values of air, acrylic plate, and metal at 25 °C. A streamlined frame flue is shown in Fig. 2 for CFD heat transfer simulations. In the chamber of the flue, The flue is then encircled with an external air skin just above ground, which creates an internal air body. To fully comprise the heat outer surface over the flue, the external air skin measures 930(width)*600(-depth)*1800(height)mm in contrast to the internal air body's quantity of 300(width)190(depth)730(height)mm. Initially, the 12 heaters were patterned as heating systems with a frequency, but the simulation's divergent conduct was poor, necessitating a trial-and-error technique to match an established empirical temp in the heating element surfaces, which is a moment process.

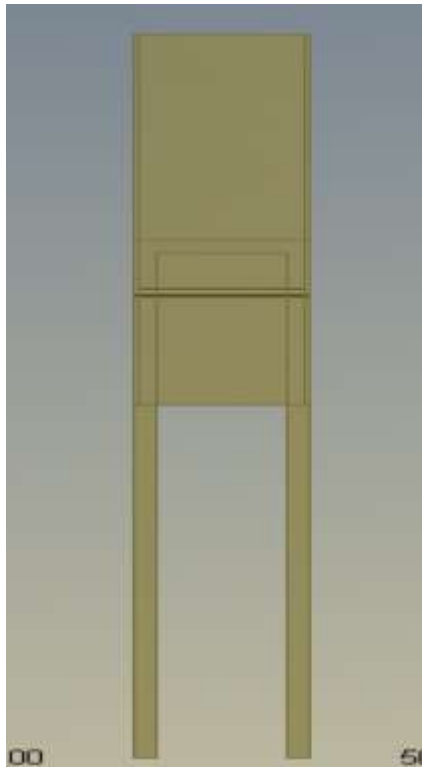


Figure 2 CAD model of Chimney



Figure 3 Mesh model of Chimney

The heating systems must eventually be deleted from the geometric shape, with their coatings contacting the internal air body rather, as seen in Leaf. 2(c) became a wall and had exploratory temperature changes assigned to them. The divergent type of behaviour was improved the quality, and the supercomputing effort was massively reduced.

Afterwards the three-dimensional Computer Aided Design configuration of the chimney is completed, it is uploaded into ANSYS workbench for more CFX assessment, and the upcoming step is meshing. Mesh is a special task wherein Computer aided configuration is segmented into huge quantities of nodes and components, and the methodology to transform into tiny chunks or components is known as meshing. To create mesh, the component dimension value is fixed to 10 mm, and the overall number of nodes created in this research is 426180, with overall number of components of 1616353, as can be seen in figure 3. Hexahedral components are employed, that are rectangle in shape and have eight nodes upon every component.

IV. RESULTS

1. The main goal of this study is to enhance the thermal effectiveness of a chimney through employing computational fluid dynamics to change the design.
2. For the temperature fluctuations within the Chimney, a computational fluid dynamics assessment was conducted on three distinct designs of Chimney.
3. For a deeper comprehension of temperature profile, 3 distinct planes were assumed: vertical, mid, and bottom.
4. The Chimney's dimensional measures are 930(width) 600(-depth) 1800(height)mm, while the internal air body's volume is 300(width) 190(depth) 730(height)mm to completely consist of the thermal boundary level across the chimney.
5. Numerous CFD analyzed data are covered in this section employing contours diagrams, data in tabular form, and form of graph.

Table 1 Meshing condition defined in various cases

	SCENARIO-1	SCENARIO-2	SCENARIO-3
NODES	426180	563354	902046
ELEMENTS	1616353	2269505	3936056

SCENARIO-1

It can be seen in the mid-plane of the Velocity contour schematic at 170oC. At the midpoint, the peak velocity is 1.024m/s as depicted in figure 4.

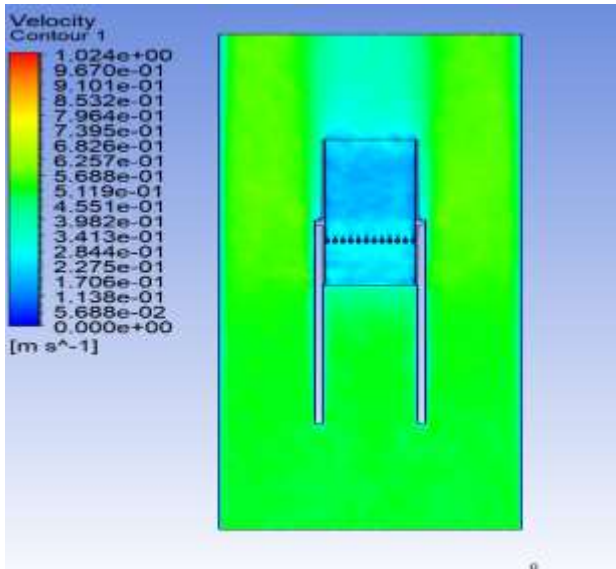


Figure 4 Velocity contours

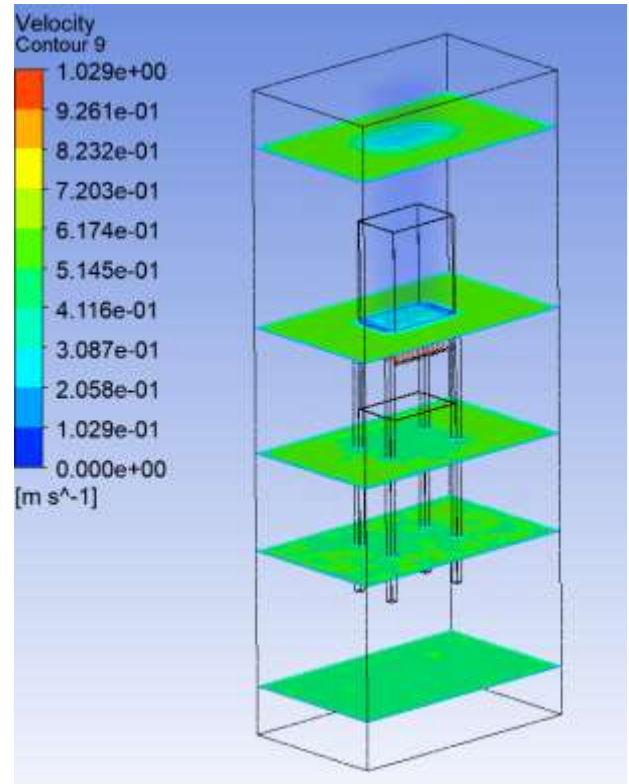


Figure 6 Velocity Contour at mid, vertical and bottom Planes

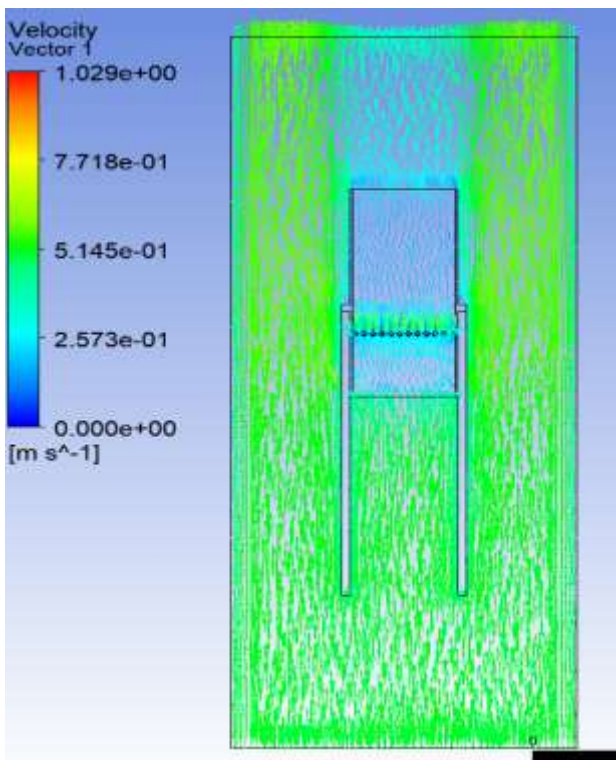


Figure 5 Velocity Vector

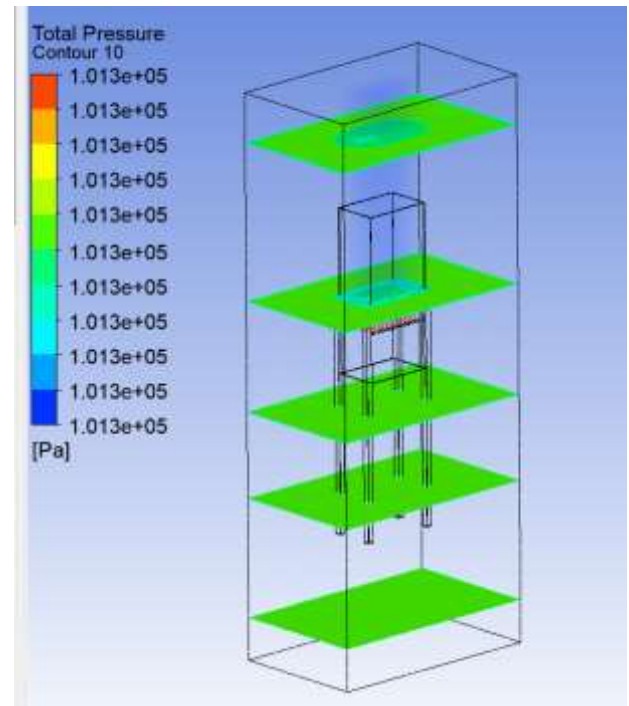


Figure 7 Pressure Contour at vertical, mid and bottom plane

It can be seen in the Eddy viscosity contour schematic at 170oC in the horizontal plane. Figure 8 shows that the peak value of Eddy viscosity at the vertical plane is 5.47E-4Pa S.

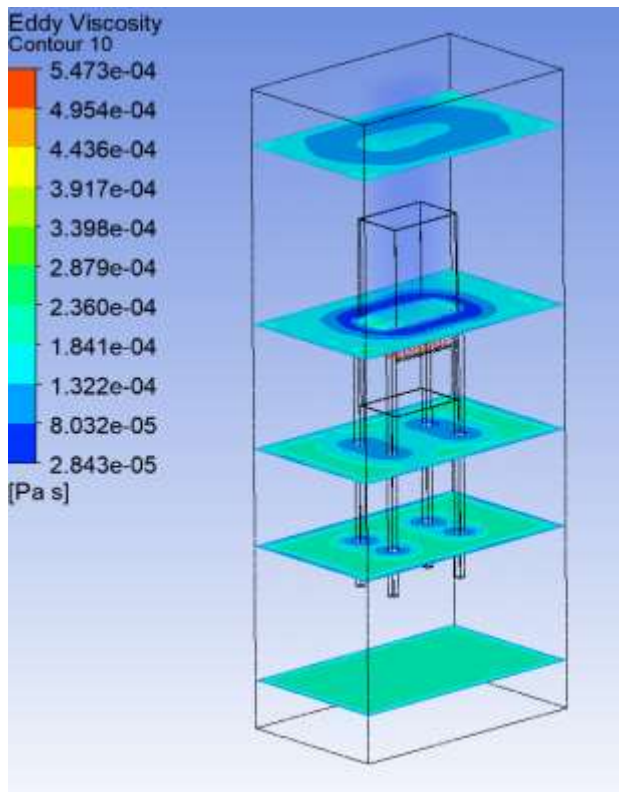


Figure 8 Eddy Viscosity Contour at vertical, mid and bottom plane

It can be seen in the temperature contour schematic at 170°C in the vertical plane. As can be seen in figure 9, the peak value of temperature at the vertical plane is 169 °C.

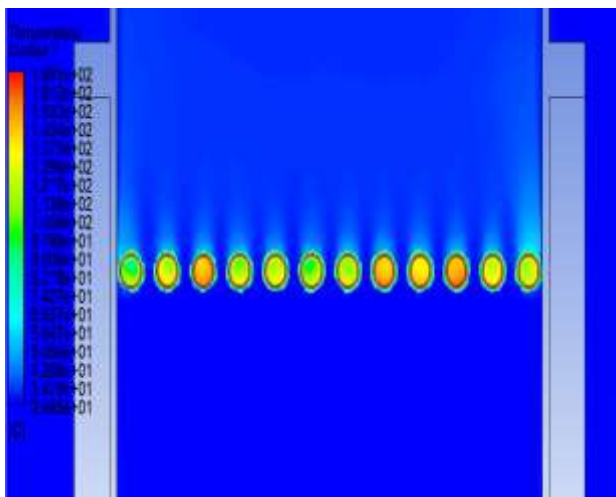


Figure 9 Temperature Contour at vertical plane

SCENARIO 2 – Similarly, It is shown in the mid-plane of the Velocity contour schematic at 170oC. The peak value of velocity at the mid plane is 1.174m/s. The temperature contour schematic at 170°C in the vertical plane. The peak value of temperature at the vertical surface is 169°C. The peak value of Eddy viscosity at the vertical surface is 4.17E-4Pa S, the Eddy viscosity contour schematic at horizontal surface at 170°C.

SCENARIO 3 - It can be seen in the mid-plane of the Velocity contour schematic at 170°C. The peak value of velocity at the mid surface is 1.496m/s. It can be seen in the temperature contour schematic at 170°C in the vertical plane. The peak value of temperature at the vertical surface is 169 °C. It can be seen in the Eddy viscosity contour schematic at 170°C in the horizontal plane. The peak value of Eddy viscosity at the vertical surface is 5.2E-4Pa S.

Table 2: Parameters in various cases

CAS ES	Velocity(m/s)	Temperature (C)	Pressure(Pa)	Eddy viscosity
1	10.24	161	101325	5.47
2	11.71	155	101325	4.7
3	14.96	141	101325	5.2

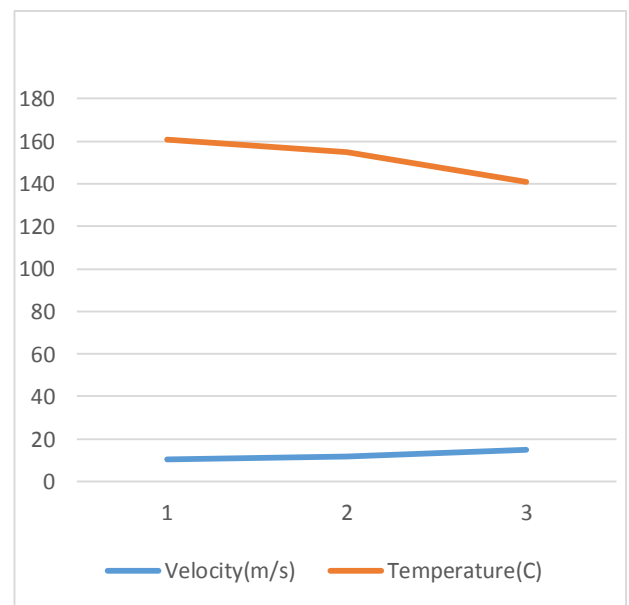


Figure 10 Variations in temperature and velocity in the given scenarios

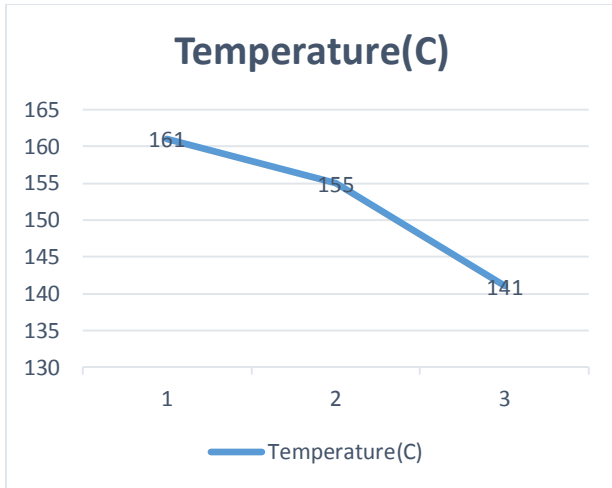


Figure 11 Temperature variation in all the three scenarios

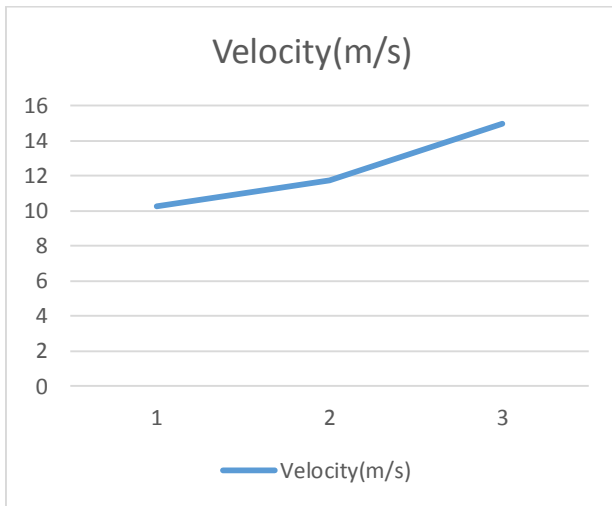


Figure 12 Velocity variation in all three scenarios

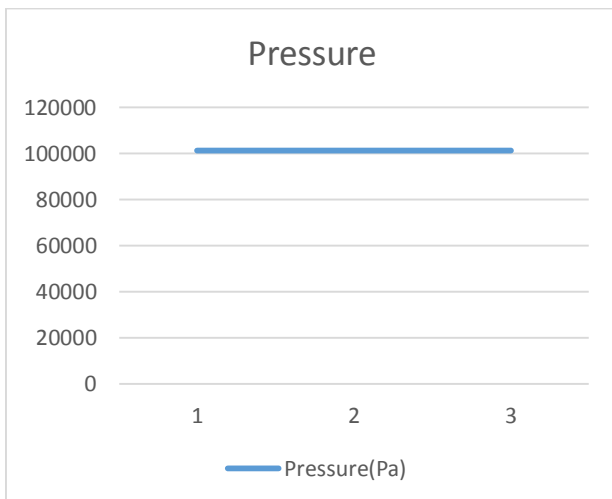


Figure 13 Pressure variation in all three scenarios

V. CONCLUSION

The system's velocity rises as the quantity of tubes increases, and the overall heat transfer rate rises as well.

- In the initial scenario, the quantity of tubes is 12, and the maximum speed is 10.24 m/s.
- In the scenario of a second maximum tube quantity of 14 and a maximum velocity of 11.71 m/s
- If the third maximum quantity is 16, and the maximum speed is 14.96 m/s.
- As the quantity of tubes increases, the radius of the tubes decreases. The maximum radius is 8mm in scenario one, 6mm in scenario two, and 4mm in scenario three.
- The system's thermal transfer rate has increased.

In scenario 3, the overall temperature reduces up to 141 degrees Fahrenheit.

- As the thermal transfer rate is increased, the system's overall performance improves.

REFERENCES

- 1) Li, W., Yu, G., Zagaglia, D., Green, R., & Yu, Z. (2020). CFD modelling of a thermal chimney for air-cooled condenser. *Geothermics*, 88(May), 101908. <https://doi.org/10.1016/j.geothermics.2020.101908>
- 2) Dhahri, M., Nekoonam, S., Hana, A., El Haj Assad, M., Arıcı, M., Sharifpur, M., & Sammouda, H. (2021). Thermal performance modeling of modified absorber wall of solar chimney-shaped channels system for building ventilation. *Journal of Thermal Analysis and Calorimetry*, 145(3), 1137–1149. <https://doi.org/10.1007/s10973-020-10248-2>
- 3) Wang, H., & Lei, C. (2020). A numerical investigation of combined solar chimney and water wall for building ventilation and thermal comfort. *Building and Environment*, 171(December 2019), 106616. <https://doi.org/10.1016/j.buildenv.2019.106616>
- 4) Khidhir, D. K., & Atrooshi, S. A. (2020). Investigation of thermal concentration effect in a modified solar chimney. *Solar Energy*, 206(May), 799–815. <https://doi.org/10.1016/j.solener.2020.06.011>
- 5) Mehdipour, R., Golzardi, S., & Baniamerian, Z. (2020). Experimental justification of poor thermal and flow performance of solar chimney by an innovative indoor experimental setup. *Renewable Energy*, 157, 1089–1101. <https://doi.org/10.1016/j.renene.2020.04.158>
- 6) Jiménez-Xamán, C., Xamán, J., Gijón-Rivera, M., Zavala-Guillén, I., Noh-Pat, F., & Simá, E. (2020). Assessing the thermal performance of a rooftop solar chimney attached to a single room. *Journal of*

- Building Engineering, 31(December 2019).
<https://doi.org/10.1016/j.jobe.2020.101380>
- 7) Sedighi, A. A., Deldoost, Z., &Karambasti, B. M. (2020). Effect of thermal energy storage layer porosity on performance of solar chimney power plant considering turbine pressure drop. *Energy*, 194, 116859.
<https://doi.org/10.1016/j.energy.2019.116859>
- 8) Azad, A., Aghaei, E., Jalali, A., & Ahmadi, P. (2021). Multi-objective optimization of a solar chimney for power generation and water desalination using neural network. *Energy Conversion and Management*, 238, 114152.
<https://doi.org/10.1016/j.enconman.2021.114152>
- 9) Nasri, F. (2020). Solar thermal drying performance analysis of banana and peach in the region of Gafsa (Tunisia). *Case Studies in Thermal Engineering*, 22(December 2019), 100771.
<https://doi.org/10.1016/j.csite.2020.100771>